AD-A039 535 RADIATION RESEARCH ASSOCIATES INC FORT WORTH TEX F/G 17/5
SOLAR INFRARED REFLECTION AND INFRARED EMISSION FROM A DUST LOA--ETC(U)
MAY 77 M B WELLS

UNCLASSIFIED RRA-M7701 AFTAC-TR-77-14 NL

1 OF 1
AD A039535

END

DATE FILMED
6-77

12

AFTAC-TR-77-14

Solar Infrared Reflection and Infrared Emission from a Dust Loaded Cloud

Radiation Research Associates, Inc.
Fort Worth, Texas

6 MAY 1977

Topical Report

Approved for public release; distribution unlimited.

Prepared for
Sandia Laboratories
Kirtland Air Force Base, NM

AIR FORCE TECHNICAL APPLICATIONS CENTER
HEADQUARTERS UNITED STATES AIR FORCE
PATRICK AIR FORCE BASE, FLORIDA 32925

UNCLASSIFIED

SECURITY CLASSIFICATION OF THIS PAGE (When Data Entered)

REPORT DOCUMENTATION PAGE	READ INSTRUCTIONS BEFORE COMPLETING FORM
1. REPORT NUMBER: AFTAC-TR-77-14	2. GOVT ACCESSION NO. / 3. RECIPIENT'S CATALOG NUMBER
4. TITLE (and Subtitle): SOLAR INFRARED REFLECTION AND INFRARED EMISSION FROM A DUST LOADED CLOUD	5. TYPE OF REPORT & PERIOD COVERED: Topical rept.
	6. PERFORMING ORG. REPORT NUMBER: RRA-M7701
7. AUTHOR(s): M. B. Wells	8. CONTRACT OR GRANT NUMBER(s): 06-0481
9. PERFORMING ORGANIZATION NAME AND ADDRESS: RADIATION RESEARCH ASSOCIATES, INC. 3550 Hulen Street Fort Worth, Texas 76107	10. PROGRAM ELEMENT, PROJECT, TASK AREA & WORK UNIT NUMBERS: Task VII
11. CONTROLLING OFFICE NAME AND ADDRESS: SANDIA LABORATORIES Kirtland Air Force Base, NM	12. REPORT DATE: 6 May 1977 / 13. NUMBER OF PAGES: 27 (28 p.)
14. MONITORING AGENCY NAME & ADDRESS (if different from Controlling Office): AIR FORCE TECHNICAL APPLICATIONS CENTER Patrick Air Force Base, FL 32925	15. SECURITY CLASS. (of this report): Unclassified / 15a. DECLASSIFICATION/DOWNGRADING SCHEDULE

16. DISTRIBUTION STATEMENT (of this Report)

Approved for public release; distribution unlimited.

17. DISTRIBUTION STATEMENT (of the abstract entered in Block 20, if different from Report)

18. SUPPLEMENTARY NOTES

Paper presented at the Annual Satellite Diagnostic Working Group Meeting Patrick AFB FL, 8-10 February 1977.

294 300.

19. KEY WORDS (Continue on reverse side if necessary and identify by block number)

Monte Carlo Methods
Radiation Transport
Dust Loaded Clouds
Infrared Radiation
Solar Radiation Reflection
Atmospheric Emission

micrometers

20. ABSTRACT (Continue on reverse side if necessary and identify by block number)

This paper presents the results of Monte Carlo calculations of reflected sunlight and air emission in the 2.653 μm to 2.760 μm wavelength band for satellite-based detectors viewing a cumulus cloud loaded with various amounts of Sahara dust positioned between 14 and 15 km altitude. The results of the calculations showed that the presence of a dust loading of $5X10^{-5}$ cm^3 of Sahara dust per m^3 of the cloud probably cannot be detected at that wavelength. Increasing the dust loading to the cloud by a factor of 100 or more gave results that indicated that the presence of the dust could be determined

cu. cm.

cubic meter

.0005

DD FORM 1 JAN 73 1473 EDITION OF 1 NOV 65 IS OBSOLETE

UNCLASSIFIED

SECURITY CLASSIFICATION OF THIS PAGE (When Data Entered)

by the use of reflected sunlight in the 2.7 μm wavelength band. Mie calculations for both the cloud and Sahara dust indicates that the best wavelength for detection of the air emission would be wavelengths near 10 μm. Additional calculations are in progress for other wavelengths in the 2 μm to 15 μm wavelength range.

MICROMETERS

TABLE OF CONTENTS

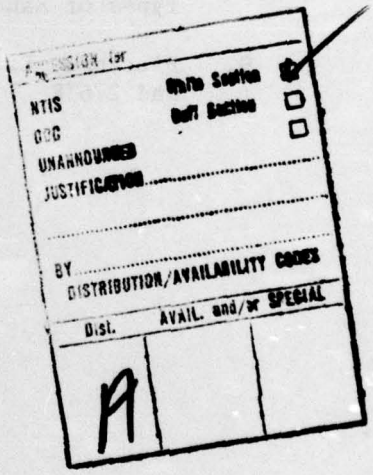

LIST OF FIGURES

LIST OF TABLES

I. INTRODUCTION

This paper presents the results of Monte Carlo studies that have been performed to determine if the presence of dust within a cloud at altitudes between 14 and 15 km could be detected at satellite altitudes. Although the purpose of the present study is to determine what wavelength intervals would be best for detection purposes, all of the Monte Carlo studies that have been performed to date have been in the 2.7 μm wavelength band. In addition, some calculations have been run with the MIE-2 procedure to obtain scattering, absorption, and extinction cross sections for both the cloud and the dust for wavelengths between 2 and 15 μm to assist in determining what wavelength intervals would be most promising for use in detection of dust-loaded clouds.

This work was perfomed under Contract Numbers 06-0481 and 06-6328 with the Sandia Laboratories. Dr. R. D. Rawcliffe of the Aerospace Corporation has contributed to the study by both suggesting the study and by defining the parameters to be used to describe both the cloud and the dust to be loaded to the cloud.

II. CALCULATIONAL METHOD

The basic computational tools being used in the study are the MIE-2 procedure (Ref. 1) and the FLASH Monte Carlo procedure (Ref. 2). The MIE-2 procedure uses MIE theory for spherical particles with a complex index of refraction and a defined particle size distribution to compute phase function data and absorption, scattering, and extinction cross section data.

FLASH is a Monte Carlo program which treats the scattering and absorption of both sunlight and air and ground emission in a spherical-shell atmosphere. FLASH is capable of treating temperature and pressure dependent absorption in the infrared by CO_2, H_2O, O_3, N_2O, CO, CH_4, and O_2 using the gaseous absorption cross section data generated by McClutchey and Shelby at the Air Force Geophysical Laboratory (Ref. 3). The restriction to these seven gases in FLASH is due only to the unavailability of data for other gases in the AFGL data base. The AFGL data are averaged over a wavenumber interval of 20 cm^{-1} and are available at 5 cm^{-1} spacings for wavenumbers between 10 cm^{-1} and 13,155 cm^{-1} (0.76 to 1000 μm). The AFGL data are input to FLASH for seven temperatures between 175° and 325°K. Data for temperatures between those used in the data base are obtained in FLASH through interpolation.

When using the AFGL data in FLASH, it is required that the wavenumber range of interest be divided into a number of intervals that are 200 cm^{-1} or less in width over which the scattering and continuum absorption cross sections can be assumed to not vary with wavenumber in each interval. Within each of these 200 cm^{-1} intervals, the effects of gaseous absorption and scattering can be calculated for up to 10 subintervals of up to 20 cm^{-1} width.

The initial effort during the first three months of the study was involved in making the FLASH procedure operational on the Sandia CDC-6600 computer system. FLASH problems were then run for a model mid-

latitude summer atmosphere containing a 15 mean-free-path thick cumulus cloud located between 14 and 15 km altitude and loaded with different amounts of dust. The wavelength range considered in the calculations uses 2.653 μm $\leq \lambda \leq$ 2.760 μm.

The atmospheric model used for these calculations was for a 25-km meteorological range in a mid-latitude summer atmosphere. The variation of the water vapor content and the temperature and pressure with altitude was obtained from measurements taken on 27 July 1973 that were previously supplied to RRA by the Air Force Technical Applications Center under another project. A 15 mean-free-path thick cumulus cloud for 2.7 μm wavelength light was positioned at altitudes between 14 and 15 km.

The altitude dependence of the atmospheric temperature as used in the FLASH calculations is shown in Fig. 1. It is seen in Fig. 1 that the atmospheric temperature has a minimum (~205°K) between 14 to 15 km altitude. It should also be noted that above the cloud the temperature reaches a maximum at an altitude of 50 km.

The particle size distribution used for the dust in the cloud was that described by the equation

$$\frac{dN}{dr} = 1.58468r^{-4.5} \quad (\mu^{-1}\ cm^{-3})$$

for Sahara dust (Ref. 4). The value of the constant in the size distribution was determined by assuming that the volume of dust in a one-m^3 volume was $5X10^{-5}$ cm^3/m^3. This resulted in a value of N = 8569.15 particles/cm^3 for dust particles with radii less than 10 μ. The index of refraction at a wavelength of 2.7 μm was taken to be 1.46 - 0.025i (Ref. 4).

The cumulus cloud was assumed to have a particle size distribution of the form (Ref. 5)

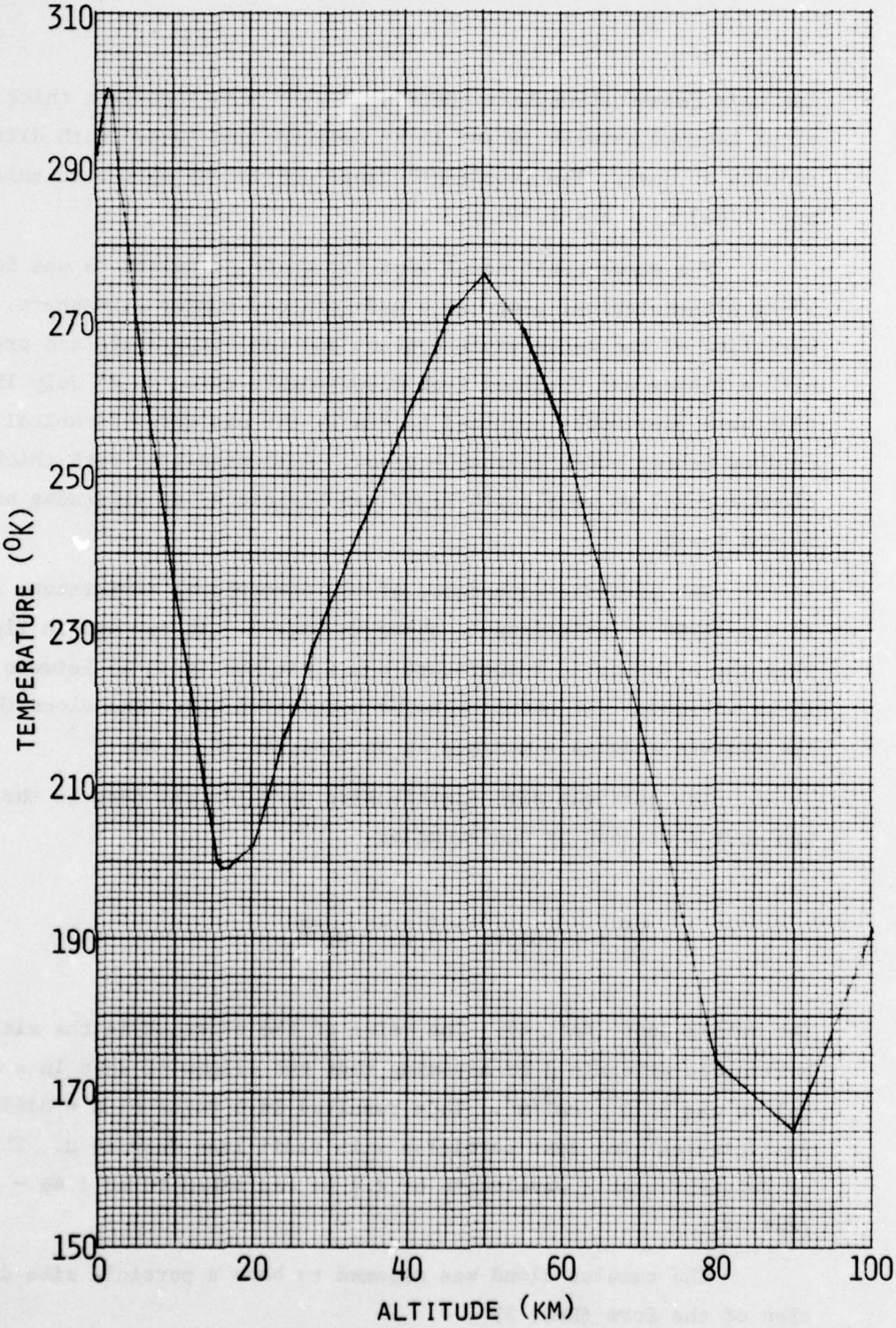

Fig. 1. Atmospheric Temperature vs Altitude

$$\frac{dN}{dr} = ar^6 e^{-1.5r} \quad .$$

The cloud droplets were assumed to be water and to have an index of refraction of 1.134 - 0.005049i (Ref. 6) for a wavelength of 2.7 μm. N was taken to be 100 particles/cm^3. The parameter a was determined by integrating the size distribution over the particle radius. The optical thickness at 2.7 μm of a one-km thick cumulus cloud was then determined from MIE calculations to be 22.166. This value was multiplied by 0.676712 to give an optical thickness of 15 for the cloud.

The extinction, scattering, and absorption optical thickness for the dust-loaded cloud are shown in Table I. These optical thicknesses do not include the absorption optical thickness resulting from gaseous absorption in the one-km thickness of the cloud. The optical thickness listed in Table I are for 1) cloud with no dust, 2) cloud with standard dust, 3) cloud with 100 times standard dust, and 4) cloud with 1000 times standard dust, where standard dust is defined by the Sahara dust distribution described above. Adding the standard dust content to the cloud resulted in a negligible change in the extinction, scattering, and absorption optical thicknesses of the cloud region. Adding 100 times and 1000 times standard dust caused noticeable increases in the optical thicknesses of the cloud region.

The geometry model used in the FLASH calculations is shown in Fig. 2. The receiver is positioned at satellite altitude and the position viewed on the top of the cloud is defined in terms of the zenith angle-of-view, θ, and the azimuthal angle ϕ between the plane containing the line-of-sight and a radial to the satellite and a plane containing the radial to the satellite and the radial to the sun. The angle θ_0 is the zenith direction to the sun at the sub-satellite point and the angle α_0 is the solar zenith angle at the point of observation at the top of the cloud.

The FLASH calculations for incident solar radiation were run for solar zenith angles of θ_0 = 0°, 10°, 30°, 50°, and 80°. The satellite

TABLE I. EXTINCTION, SCATTERING AND ABSORPTION OPTICAL THICKNESSES USED FOR CLOUD REGION BETWEEN 14 AND 15 KM ALTITUDE

MODEL	ρ_T	ρ_s	ρ_a
CLOUD WITHOUT DUST	15.00	13.8864	1.11360
CLOUD WITH STANDARD DUST	15.019996	13.900553	1.11944
CLOUD WITH 10^2 X STANDARD DUST	17.039983	15.348935	1.6910479
CLOUD WITH 10^3 X STANDARD DUST	35.389989	28.504513	6.8854757

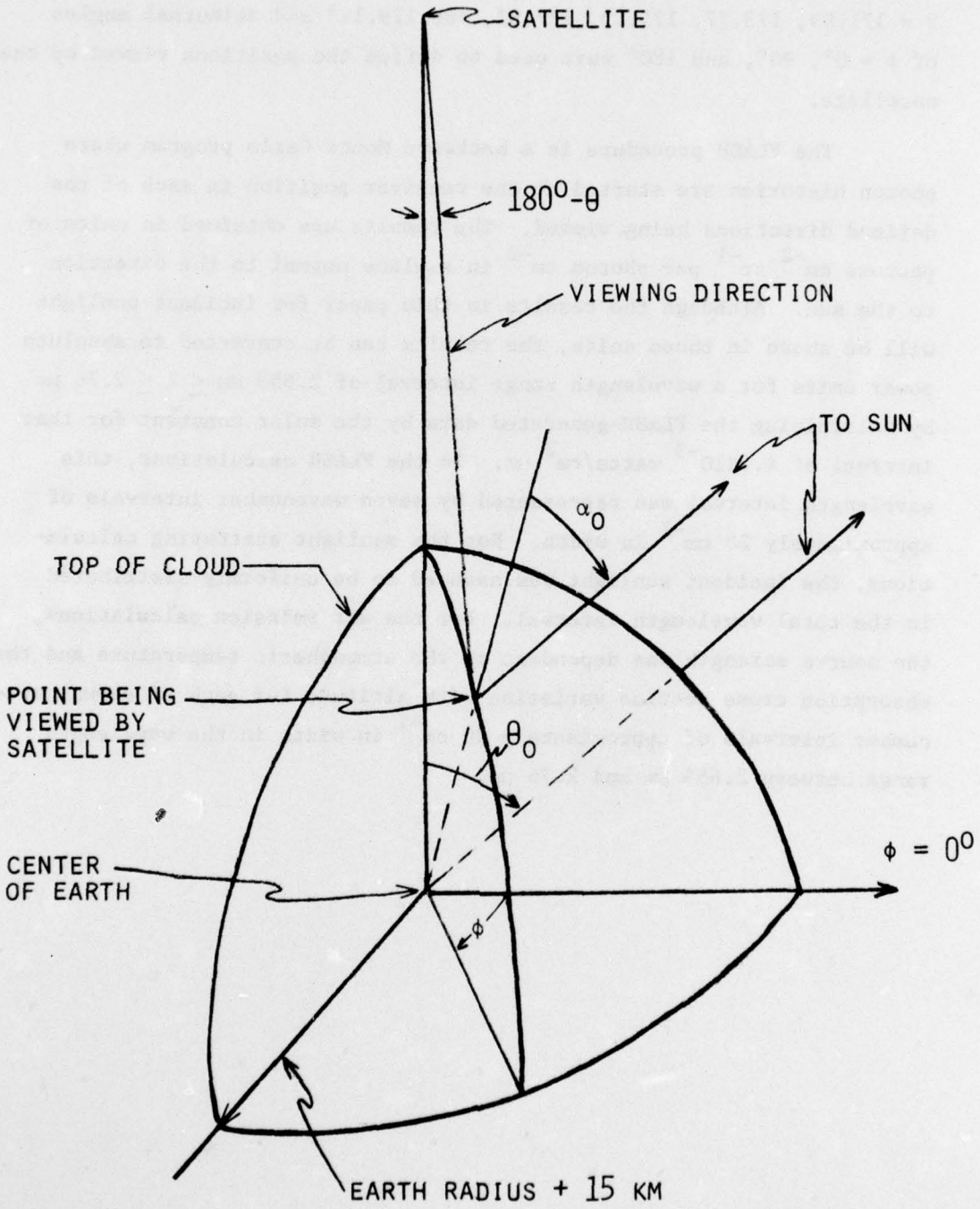

Fig. 2. Geometry Used in Monte Carlo Calculations

altitude was taken to be 35,800 km. Receiver zenith view angles of θ = 171.99, 173.77, 175.55, 177.33, and 179.11° and azimuthal angles of ϕ = 0°, 90°, and 180° were used to define the positions viewed by the satellite.

The FLASH procedure is a backward Monte Carlo program where photon histories are started at the receiver position in each of the defined directions being viewed. The results are obtained in units of photons cm^{-2} sr^{-1} per photon cm^{-2} in a plane normal to the direction to the sun. Although the results in this paper for incident sunlight will be shown in those units, the results can be converted to absolute power units for a wavelength range interval of 2.653 μm $\leq \lambda \leq$ 2.76 μm by multiplying the FLASH-generated data by the solar constant for that interval of $4.3X10^{-3}$ watts/cm^2 μm. In the FLASH calculations, this wavelength interval was represented by seven wavenumber intervals of approximately 20 cm^{-1} in width. For the sunlight scattering calculations, the incident sunlight was assumed to be uniformly distributed in the total wavelength interval. For the air emission calculations, the source strength was dependent on the atmospheric temperature and the absorption cross section variation with altitude for each of seven wavenumber intervals of approximately 20 cm^{-1} in width in the wavelength range between 2.653 μm and 2.76 μm.

III. CALCULATIONAL RESULTS

The dependence of the magnitude of the scattered solar radiation at the satellite on the number of collisions followed in the Monte Carlo calculations was examined to insure that the calculations were carried out to a large enough number of collisions so that the results would not be underestimates of the scattered radiation intensity. Figure 3 shows results typical of that obtained when the cloud did not contain any dust. The results shown are for a receiver zenith angle of view of 171.99°, and azimuthal angle of 0°, and for solar zenith angles at the sub-satellite point of 0° and 10°. It was found that contributions to the scattered intensity from collisions greater than 20 (that used in the Monte Carlo calculations) would not contribute significantly to the total scattered intensity.

Figure 4 shows similar type data for the case where the cloud was loaded with a dust content equal to 1000 times the standard dust amount. The results shown are for solar zenith angles $\theta_0 = 0°$ and 30° and the receiver was looking in a direction defined by $\theta = 179.11°$ and $\phi = 0°$. The scattered intensity falls off approximately exponentially with collision number and the contribution from collisions greater than 20 was estimated to be negligible for those cases.

The variation of the reflected sunlight intensity at the satellite when the satellite zenith angle of view is 179.11° is shown in Fig. 5 for cases where the azimuthal direction of view, ϕ, is either 0° or 90°. The data are plotted in Fig. 5 versus the solar zenith angle θ_0 at the sub-satellite point. It is seen that there is clearly a difference in the magnitude of the reflected radiation when the cloud is loaded with 100 times and 1000 times the standard dust. The statistics of the Monte Carlo data for the cases where the cloud contained no dust and where it contained the standard dust loading are not good enough to say with certainty that a detector would see a difference in the reflected radiation for those cases.

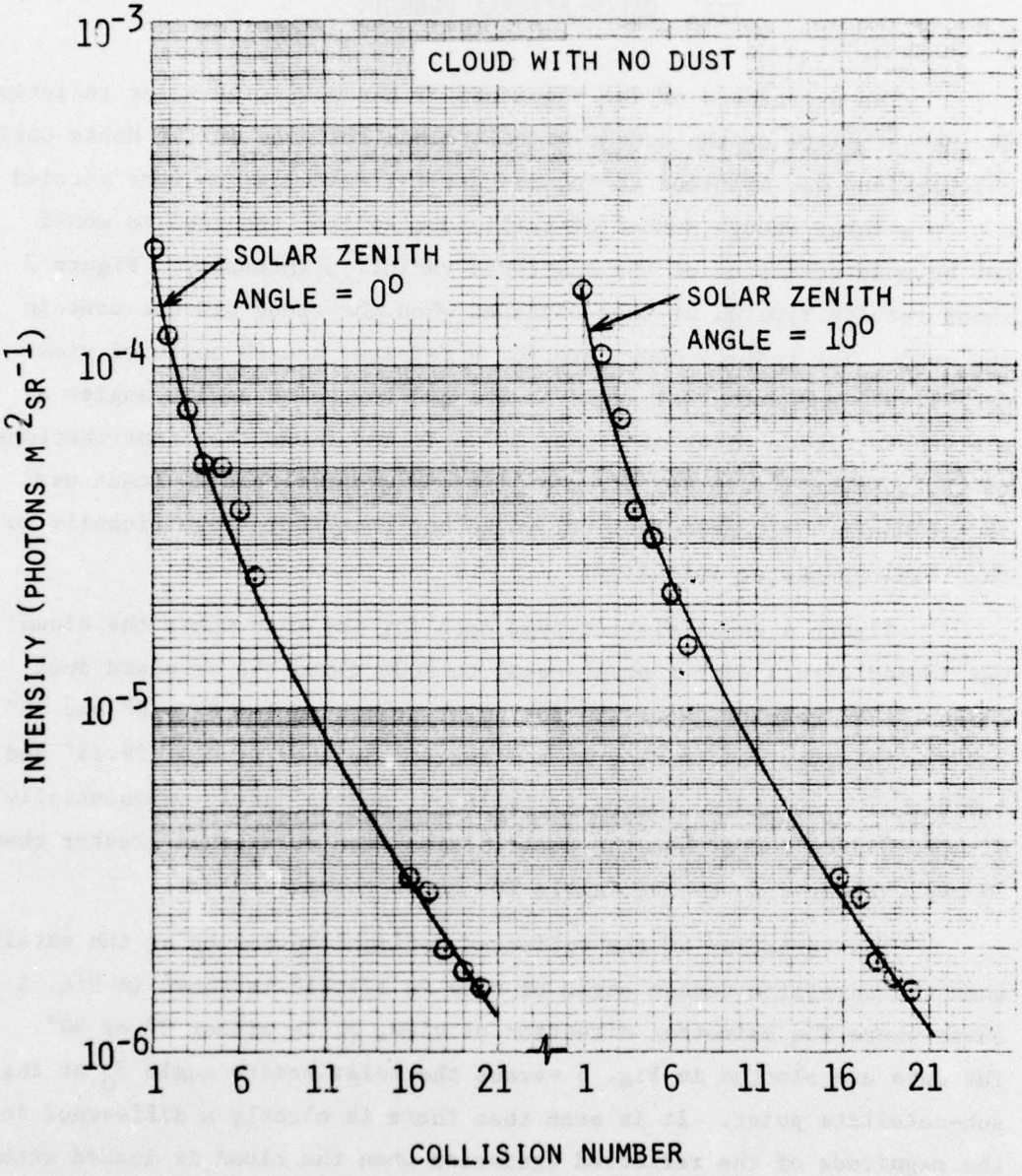

Fig. 3. Reflected Intensity for $\theta = 171.99°$ and $\phi = 90°$

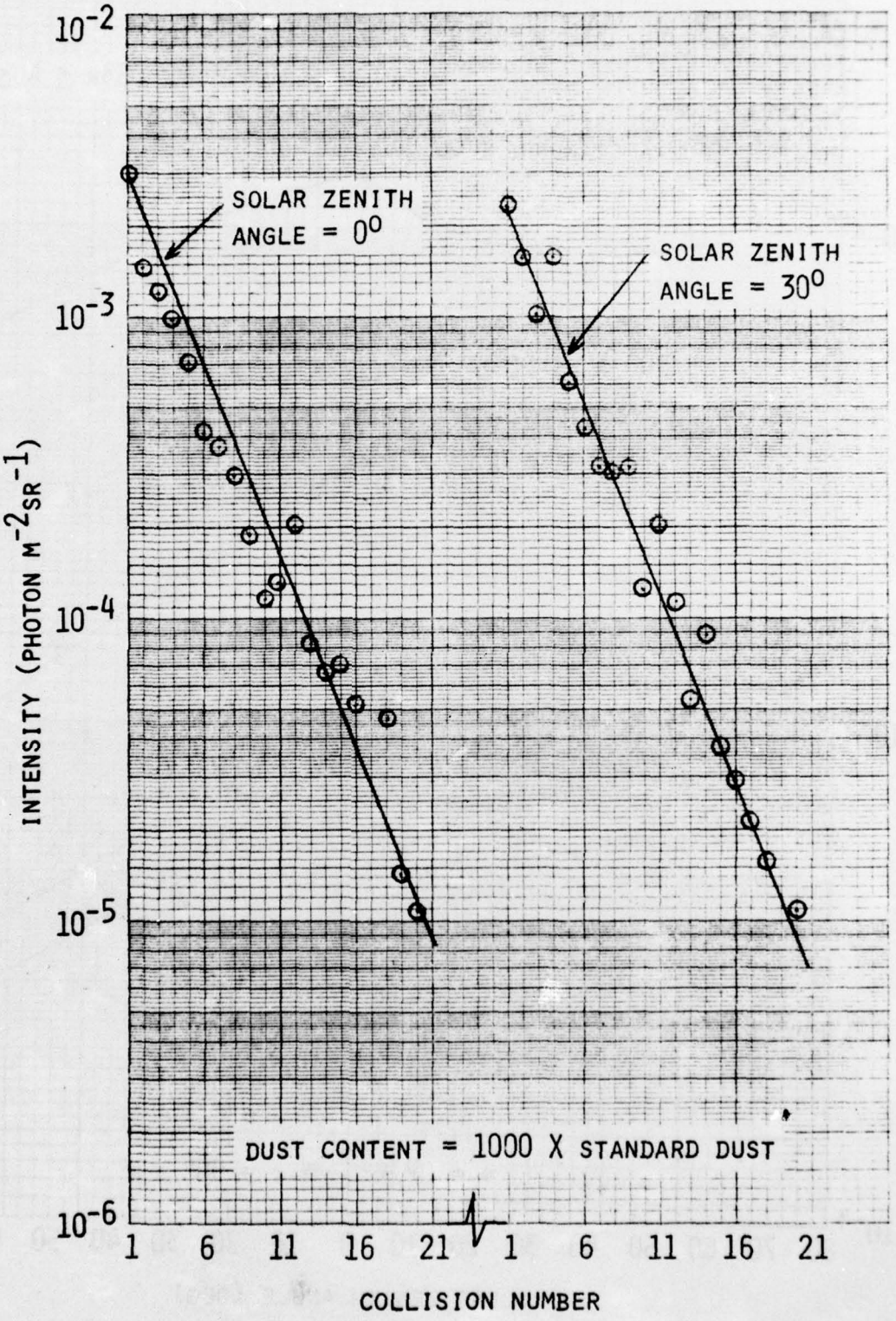

Fig. 4. Reflected Intensity for $\theta = 179.11°$ and $\phi = 0°$

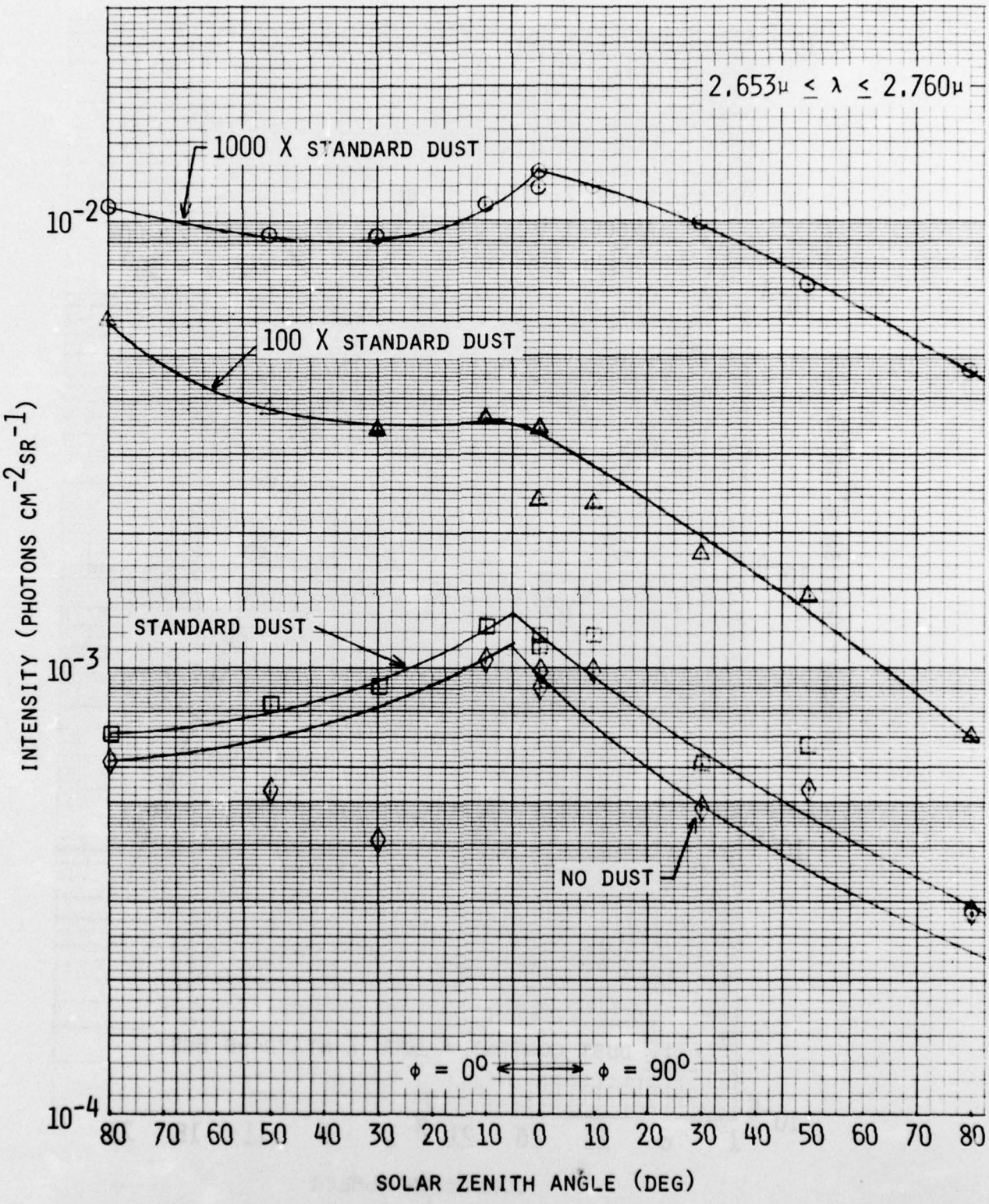

Fig. 5. Reflected Sunlight for θ = 179.11°

Figure 6 shows similar data for reflected sunlight when the receiver zenith angle of view is 171.99°. For this receiver zenith angle of view, it is seen that there is a significant difference in the magnitude of the backscattered intensity for the cases where the cloud contains 100 and 1000 times the standard dust loading. As pointed out in the previous figure, it is doubtful that the presence of standard dust could be determined with respect to the reflected radiation from clouds with no dust or clouds loaded with standard dust. For this satellite zenith angle of view and for a azimuthal view angle of $\phi = 0°$, a satellite would probably have difficulty determining if the cloud contained as much as 100 times standard dust when the solar zenith angle θ_0 is greater than about 45°.

A tabulation of the air emission signal at the satellite in the 2.653 to 2.760 μm wavelength interval as a function of dust content and satellite zenith angle of view is shown in Table II. The upper part of Table II shows the total intensity from all of the atmosphere in the direction being viewed and the lower part of Table II shows the intensity from air emission in only the atmospheric layer containing the cloud. In general, the infrared energy at the satellite in a given viewing direction does not change when either standard dust or 100 times standard dust is added to the cloud. Increasing the dust content in the cloud to 1000 times standard dust does result in a slight decrease in the air emission reaching the detector in a given viewing direction over that obtained for the other dust contents considered. In general, only about 30% of the energy at the detector in a given viewing direction comes from the cloud layer.

Table III shows that the total intensity of air-emitted radiation at the detector in a given direction from only the cloud layer is approximately a factor of 4 to 6.7 larger than the intensity of air-emitted radiation which gets to the receiver from the cloud without undergoing scattering in the cloud or the upper atmosphere.

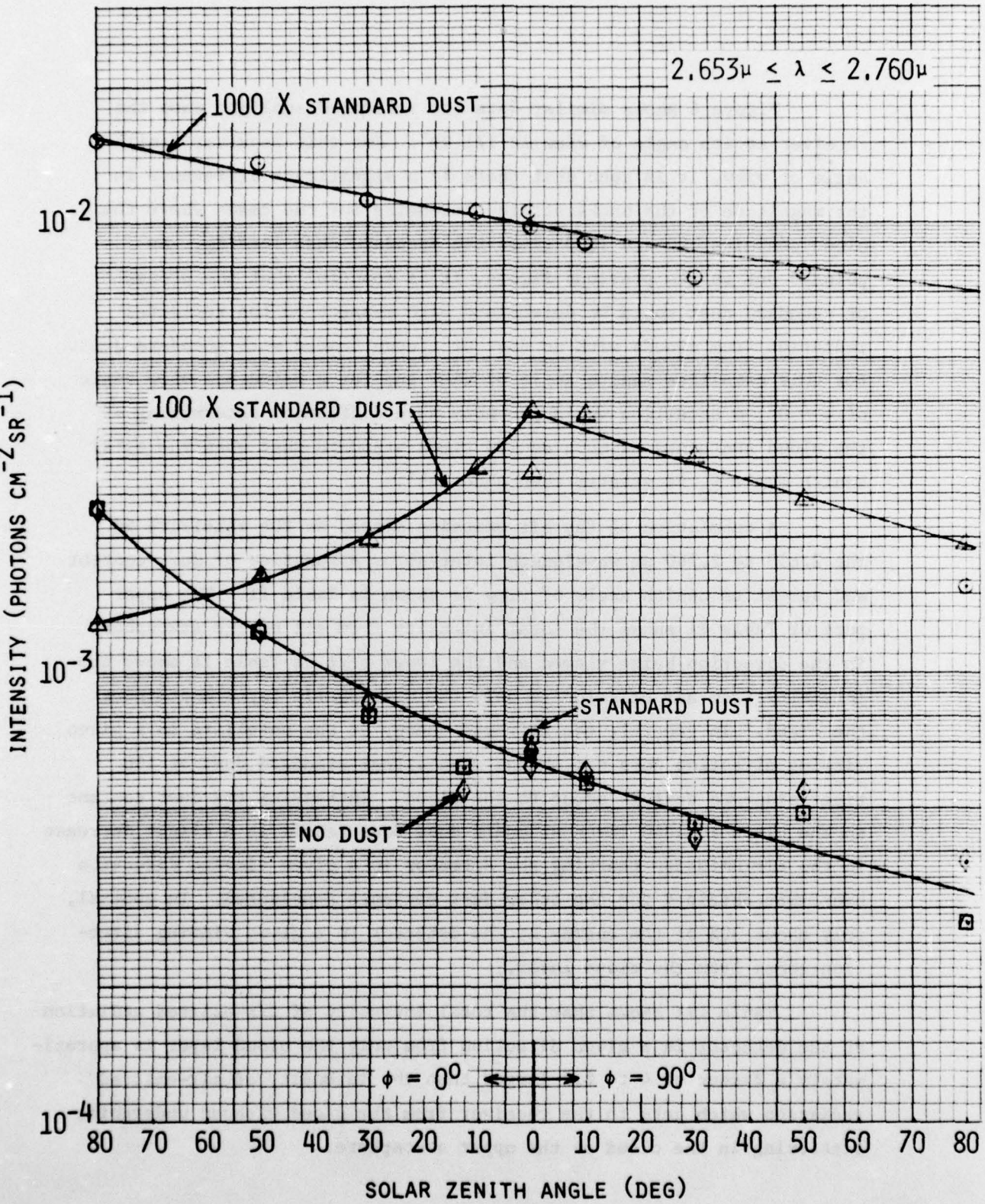

Fig. 6. Reflected Sunlight for θ = 171.99°

TABLE II. ENERGY AT SATELLITE FROM AIR EMISSION

TOTAL AIR EMISSION (WATTS $M^{-2}\mu M^{-1}SR^{-1}$)

DUST CONTENT	SATELLITE VIEWING ANGLE (DEG)				
	171.99	173.77	175.55	177.33	179.11
NO DUST	7.708-5	6.416-5	5.951-5	5.816-5	5.733-5
STANDARD DUST	7.663-5	6.416-5	5.950-5	5.828-5	5.731-5
10^2 STAND. DUST	5.076-5	6.432-5	6.019-5	5.784-5	5.760-5
10^3 STAND. DUST	6.984-5	5.878-5	5.586-5	5.395-5	5.378-5

EMISSION FROM CLOUD ONLY (WATTS $M^{-2}\mu M^{-1}SR^{-1}$)

DUST CONTENT	SATELLITE VIEWING ANGLE (DEG)				
	171.99	173.77	175.55	177.33	179.11
NO DUST	1.951-5	2.042-5	1.911-5	1.842-5	1.823-5
STANDARD DUST	1.941-5	2.043-5	1.913-5	1.844-5	1.827-5
10^2 STAND. DUST	1.893-5	2.073-5	2.083-5	2.007-5	2.011-5
10^3 STAND. DUST	1.250-5	1.512-5	1.552-5	1.644-5	1.699-5

TABLE III. IMPORTANCE OF SCATTERING FOR AIR EMISSION IN THE 2.7 μM BAND FROM CLOUD ONLY

(DIRECT PLUS SCATTERED/DIRECT)

DUST CONTENT	SATELLITE VIEWING ANGLE (DEG)				
	171.99	173.77	175.55	177.33	179.11
NO DUST	6.3	6.7	6.5	6.5	6.5
STANDARD DUST	6.1	6.6	6.5	6.5	6.5
10^2 STAND. DUST	5.7	5.9	6.1	5.9	6.0
10^3 STAND. DUST	3.7	4.0	3.9	4.1	4.2

The results obtained from the FLASH calculations for both the reflected sunlight and the air-emission radiation at the satellite indicate that it is doubtful that one would be able to determine that a cloud has been loaded with an amount equal to that assumed for standard dust when the detector is viewing infrared radiation in the 2.653 to 2.760 μm wavelength range.

Since the results shown in Figs. 5 and 6 and Table II were obtained, we have performed some additional MIE-2 calculations in an effort to determine what infrared radiation wavelength interval offers the best possibility of being able to detect the presence of dust in high altitude clouds. In the preliminary study described above, the cumulus cloud particles were assumed to be water droplets. Since the cloud was assumed to be located between 14 and 15 km altitude, where the atmospheric temperature is a minimum, we decided to assume that the cloud was made up of ice particles. The indices of refraction for ice particles were taken from Ref. 7. Figure 7 shows the absorption, scattering, and extinction cross sections computed with Mie theory for the cumulus cloud, assuming ice particles. The optical thickness of the cloud at a wavelength of 0.55 μm is 16.6 for a 1.0 km-thick cloud. Figure 8 shows the absorption and extinction coefficients for the standard amount of dust for cases where the dust distribution is defined either with a $r^{-3.5}$ or an $r^{-4.5}$ distribution. In both cases, the total volume of dust was taken to be 5.0×10^{-11} cm^3/cm^3. It is noted in Fig. 7 that a minimum in the extinction coefficient for the cloud occurs at 10 μm. It is also to be noted in Fig. 8 that a maximum in the absorption and extinction coefficients for Sahara dust also occurs at wavelengths near 10 μm. At a 10-μm wavelength the absorption optical thickness in the cloud with standard dust will be greater than it was at 2.7 μm but the total optical thickness will be less. The emission from the cloud with dust is dependent on the magnitude of the absorption cross section and the wavelength. The blackbody emittances as given by Planck's law for temperatures of 207.5°K and 276°K are shown in Fig. 9 as a function of wavelength. The 207.5°K temperature is the

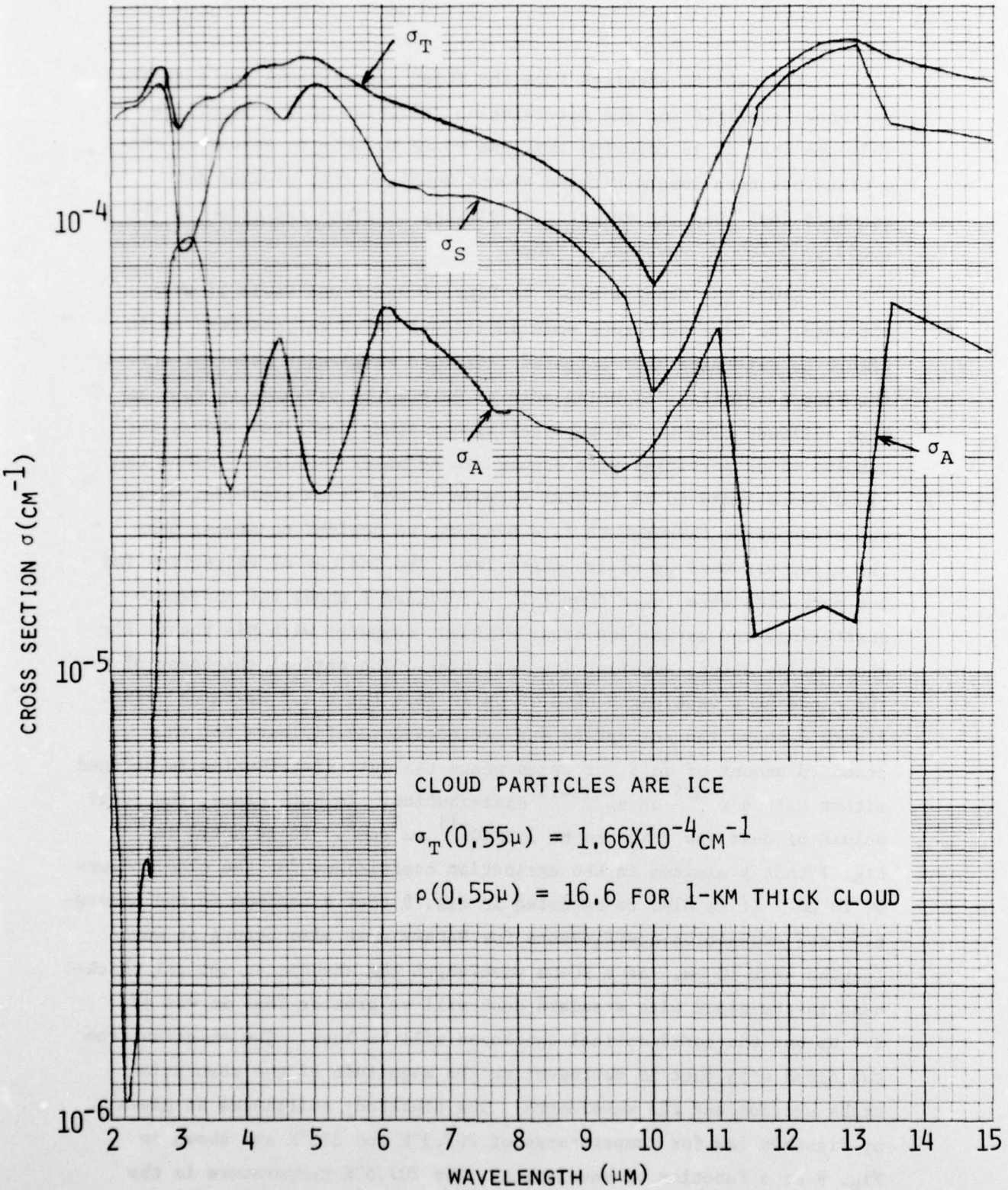

Fig. 7. Cumulus Cloud Cross Sections

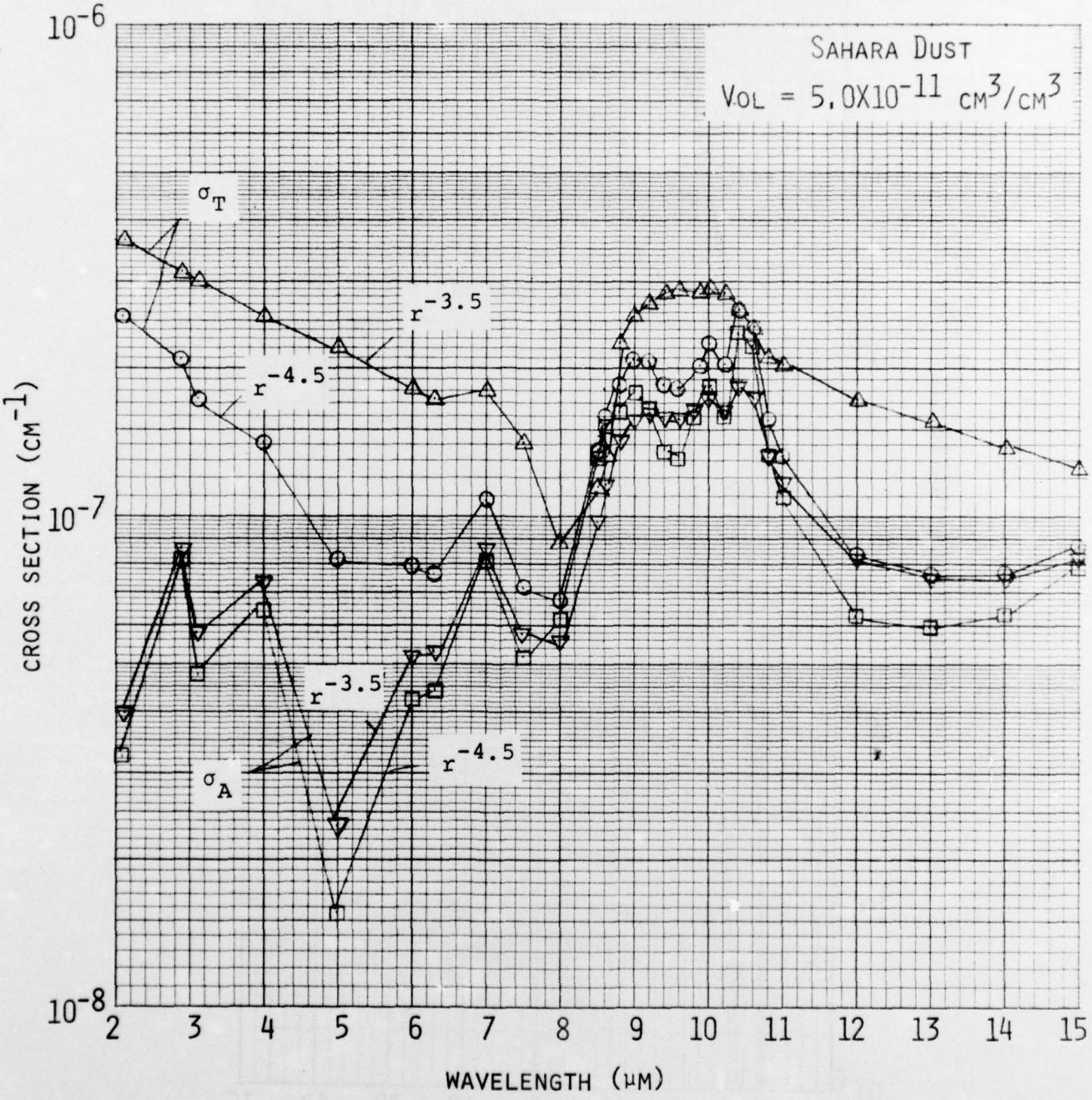

Fig. 8. Absorption and Extinction Cross Sections for Two Types of Sahara Dust Distributions

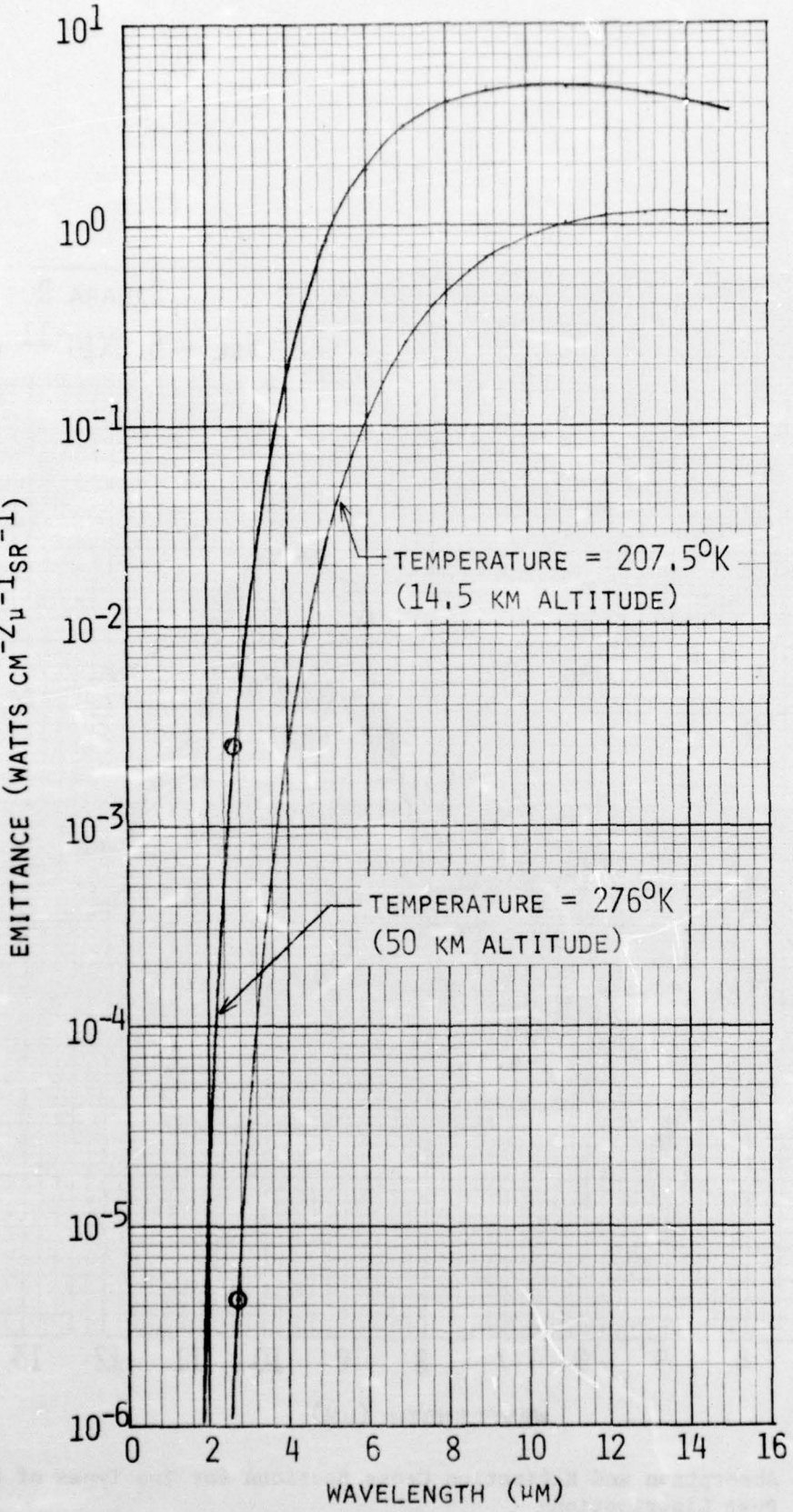

Fig. 9. Blackbody Emittance for Temperatures of 207.5°K and 276°K

average temperature of the cloud and 276°K is the maximum temperature which occurs at 50 km altitude. For the 2.7 μm wavelength, Planck's law shows that there is a factor 580 more energy emitted at a temperature of 276°K than there is at a temperature of 207.5°K. Increasing the wavelength of emission to 10.0 μm results in a much larger increase in the magnitude of the blackbody emittance as given by Planck's law. In addition, the emittance at a wavelength of 10.0 μm for a temperature of 276°K is only a factor of 5.88 greater than the emission at a wavelength of 10.0 μm when the atmosphere is at a temperature of 207.5°K.

In the next few months, RRA plans to run FLASH calculations at other wavelengths for both reflected solar radiation and air emission to see if there are wavelengths for which it is possible to differentiate between clouds that contain either standard dust or no dust.

REFERENCES

1. Wolfram G. Blättner, Utilization Instructions for Operation of the MIE-2 Program on the Sandia CDC-6600 Computer, Radiation Research Associates, Inc. Research Note RRA-N7513 (September 1975)

2. Wolfram G. Blättner, Utilization Instructions for the FLASH Monte Carlo Procedure, Radiation Research Associates, Inc. Research Note RRA-N7512 (August 1975)

3. R. A. McClatchey, private communication, 1974

4. F. Volz, "IR Optical Constants of Ammonium Sulphate, Sahara Dust, Volcanic Pumice and Flyash", Appl. Opt., Vol. 12, No. 3, p. 564 (1973)

5. D. Deirmendjian, Electromagnetic Scattering on Spherical Polydispersions, Elsevier, New York (1969)

6. G. M. Hale and M. R. Querry, "Optical Constants of Water in the 200 nm to 200 μm Wavelength Region", Appl. Opt., Vol. 12, No. 3, p. 555 (1973)

7. W. Irvine and J. Pollack, "Infrared Optical Properties of Water and Ice Spheres", Icarus (1967)

DISTRIBUTION

No of Copies	
	DOD AGENCIES
2	Director Defense Nuclear Agency ATTN: RAAE Technical Library
2	Director Defense Intelligence Agency ATTN: Nuclear Energy Division Technical Library
12	Defense Documentation Center ATTN: Document Control
2	Director Defense Advanced REsearch Projects Agency ATTN: NMRO TIO
	ENERGY RESEARCH AND DEVELOPMENT ADMINISTRATION
5	Los Alamos Scientific Laboratory ATTN: J-10 (Dr H. Horak) J-10 (Dr Guy Barasch) T-12 (Dr D.C. Cartwright) TD-3 (Dr Bob Henson) Technical Library
1	ERDA/DMA ATTN: Mr D. Gale
3	Sandia Laboratories ATTN: Dean Thornbrough Bob Bradley Reports Collection
1	Lawrence Livermore Laboratory ATTN: Technical Library
1	Oak Ridge National Laboratory ATTN: Technical Library
1	EG&G, Inc. Bedford MA ATTN: Technical Library
1	EG&G, Inc. Los Alamos NM ATTN: Dr C. Mitchell
	DEPARTMENT OF THE ARMY
1	Army Nuclear Effects Lab ATTN: Technical Library
2	US Army Electronics Command ATTN: Technical Library Dr. R. Buser
1	US Army Combat Developments Command-Institute of Nuclear Studies ATTN: Technical Library
2	US Army Waterways Experiment Station-Mobility and Environmental System Lab ATTN: Dr. L.E. Link Dr. Warren Grabau
3	US Army Electronics Command Atmospheric Sciences Laboratory ATTN: Dr M.L. Vatsia Dr Jerry Lentz Dr Richard Gomez
1	US Army Missile and Development Command-Physical Sciences Directorate ATTN: Dr Julius Lilly
2	Ballistic Research Laboratory ATTN: Mr. Norman Banks Mr. Ennis Quigley

No of Copies	
	DEPARTMENT OF THE NAVY
1	Naval Research Laboratory ATTN: Technical Library
1	Naval Postgraduate School ATTN: Technical Reports Librarian
2	Naval Surface Weapons Center ATTN: Mr Williard Derksen Mr Barry Katz
1	Naval Ordnance Test Station ATTN: Dr. Richard Bird
	DEPARTMENT OF THE AIR FORCE
4	AF Geophysics Laboratories ATTN: OPR (Mr H. Gardiner) OPA (Dr R. Fenn) OPR (Dr A. T. Stair) Research Library
1	AF Institute of Technology ATTN: Library
4	AF Weapons Laboratory ATTN: Dr Joe Janni Mr Al Sharp Dr C. Needham Technical Library
1	Space and Missile Systems Organization ATTN: SZS (Maj H. Hayden)
2	AF Technical Applications Center ATTN: TFR (Capt J. Lange)
1	AFETAC ATTN: DNE (Capt L. Mendenhall)

No of Copies	
	DOD CONTRACTORS
3	Aerospace Corporation ATTN: Dr R.D. Rawcliffe Dr Kelly Spearman Library Services
1	Analytical Systems Corporation ATTN: Dr I. Kohlberg
1	Battelle Memorial Institute ATTN: Radiation Effects Information Center
1	AVCO - Everett Research Laboratory ATTN: Technical Library
1	General Electric Company-TEMPO ATTN: DNA Information and Analysis Center
1	Kaman Sciences Corporation Kaman Nuclear Division ATTN: Technical Library
1	Lockheed Missiles and Space Company ATTN: Technical Library
1	The MITRE Corporation ATTN: Technical Library
1	The RAND Corporation ATTN: Technical Library
1	R&D Associates ATTN: Technical Library
1	Stanford Research Institute ATTN: Technical Library

No of Copies	
1	TRW Systems Group ATTN: Technical Information Center
1	Visidyne, Inc. ATTN: Dr. J. Carpenter
1	Mission Research Corporation ATTN: Technical Library
1	Teledyne Brown Engineering
1	Science Applications, Inc. ATTN: Dr R. Hillendahl
1	HSS, Inc. ATTN: Dr H. Stewart
20	Radiation Research Associates ATTN: M.B. Wells
1	Bendix Engineering Corporation Grand Junction Operations ATTN: Dr Peter Alexander
1	Institute for Defense Analyses ATTN: Technical Information Office